AJNR

Elastase-Induced Saccular Aneurysms in Rabbits: Comparison of Geometric Features with Those of Human Aneurysms

John G. Short, Naomi H. Fujiwara, William F. Marx, Gregory A. Helm, Harry J. Cloft and David F. Kallmes

AJNR Am J Neuroradiol 2001, 22 (10) 1833-1837
http://www.ajnr.org/content/22/10/1833

AJNR Am J Neuroradiol 22:1833–1837, November/December 2001

Elastase-Induced Saccular Aneurysms in Rabbits: Comparison of Geometric Features with Those of Human Aneurysms

John G. Short, Naomi H. Fujiwara, William F. Marx, Gregory A. Helm, Harry J. Cloft, and David F. Kallmes

BACKGROUND AND PURPOSE: **The development of more effective intracranial aneurysm therapy depends on the ability to test various intravascular occlusion devices and techniques in preclinical animal models. This requires the creation of experimental aneurysms, which, ideally, should mimic the size and geometric features of human intracranial aneurysms. The purpose of this study was to characterize the morphologic features of elastase-induced saccular aneurysms in rabbits to determine whether the morphology of such aneurysms mimics that of human intracranial aneurysms.**

METHODS: **Elastase-induced saccular aneurysms were created in 40 New Zealand white rabbits. Intravenous digital subtraction angiography was performed 14 days after surgery. Relative to an external sizing device, the following dimensions were determined: aneurysm dome (height and width), aneurysm neck diameter, and parent artery diameter. Based on maximal diameter, aneurysms were categorized as small (2.0–4.9 mm), medium-sized (5.0–9.9 mm), or large (10–16 mm), and as narrow-necked (<4.0 mm neck width) or wide-necked (>4.0 mm neck width). Mean dome-neck ratio was calculated and compared with that of human aneurysms.**

RESULTS: **All aneurysm cavities were angiographically patent. Widths of the cavities ranged from 2.5 to 7.1 mm (mean, 4.1 ± 1.2 mm); heights ranged from 3.0 to 15.6 mm (mean, 8.8 ± 2.6 mm). Three (7.5%) of 40 aneurysms were small, 20 (50%) were medium-sized, and 17 (42.5%) were large. Twenty-two (55%) of 40 aneurysms were small-necked, and 18 (45%) were wide-necked. Mean dome-neck ratio was 1.13 ± 0.54. Mean parent artery diameter was 4.3 ± 1.4 mm.**

CONCLUSION: **Saccular aneurysms of sizes similar to that of human intracranial aneurysms were reliably created using a simple method of vessel ligation and elastase injury. Neck sizes varied with both large and small-necked aneurysms created.**

Increasing numbers of patients with cerebral aneurysms are being treated by endovascular techniques using Guglielmi detachable coils (GDCs). While immediate aneurysm obliteration is frequently obtained, the long-term durability of this technique is still being defined, with reports of aneurysm recurrence rates as high as 14%, even in totally occluded aneurysms (1).

Received October 9, 2000; accepted after revision June 8, 2001.

From the Departments of Radiology (J.G.S., N.H.F., W.F.M., D.F.K.) and Neurosurgery (G.A.H.), University of Virginia Health Services, Charlottesville; and the Department of Radiology, Emory University Hospital, Atlanta, GA (H.J.C.).

Address reprint requests to John G. Short, MD, Box 170, Department of Radiology, University of Virginia Health Services, Charlottesville, VA 22908.

The development of more effective intracranial aneurysm therapy depends on the ability to test various intravascular occlusion devices and techniques in preclinical animal models. Several methods of experimental creation of saccular aneurysms have been described (2–7). Experimental aneurysms would ideally mimic the size and geometric features of human intracranial aneurysms, not only in terms of aneurysm diameter but also regarding the width of the aneurysm neck. Experimental aneurysms should also have sufficient variability in dome and neck size to test various endovascular techniques of occlusion. Finally, experimental aneurysms should have biological characteristics that simulate the biological processes seen in human aneurysms both before and after therapy.

A new method for creation of elastase-induced arterial saccular aneurysms in rabbits by using endovascular techniques has recently been described (3, 8, 9). In the current study, we report the results

of a detailed examination of the size and geometric features of 40 consecutive experimental aneurysms created with the use of this new technique and compare the morphologic and size characteristics of these experimental aneurysms with those of human aneurysms. We propose that the data presented will help determine whether this new aneurysm model reliably provides aneurysm cavities appropriate in size for preclinical testing of aneurysm occlusion devices and techniques.

Methods

Aneurysm Creation

Aneurysms were created in New Zealand white rabbits (3–4 kg) with approval of the animal review committee at our institution. The technique used for creation of elastase-induced aneurysms has previously been described in detail (8). Briefly, anesthesia was induced by intramuscular injection of 60 mg/kg ketamine (Ketaved; Vedco, St. Joseph, MO) and 6 mg/kg xylazine (Traquived; Vedco). The right common carotid artery (CCA) was surgically exposed and ligated distally with 3–0 silk suture. A small arteriotomy was performed, and a 5F vascular sheath (Cordis Endovascular, Miami Lakes, FL) with a beveled tip was advanced in a retrograde manner into the mid portion of the CCA. Through the diaphragm of the sheath, a 3F Fogarty balloon (Baxter Healthcare Corp, Irvine, CA) catheter as well as a Tracker 10 microcatheter (Target Therapeutics, Fremont, CA) were introduced into the CCA. The balloon was positioned within the brachiocephalic artery at the origin of the right CCA, and the tip of the microcatheter was positioned immediately cephalad to the balloon, to reside at the origin of the CCA. The balloon was gently inflated to effect occlusion of the brachiocephalic artery and the origin of the CCA.

A solution of 25% by volume normal saline, 25% by volume iodinated contrast material (Omnipaque 300; Nycomed, Princeton, NJ), and 50% by volume porcine elastase (5.23 U/mgP, 40.1 mgP/mL; Worthington Biochemical Corp, Lakewood, NJ) was prepared on the bench. Under continuous fluoroscopic monitoring, this saline-contrast-elastase solution was infused into the lumen of the microcatheter until the lumen of the CCA was slightly expanded in size, but care was taken to stop the injection before the solution leaked into the brachiocephalic artery around the Fogarty balloon. The solution was maintained in place within the lumen of the CCA for 10 minutes. Subsequently, the balloon catheter, microcatheter, and sheath were removed. The CCA was ligated and the skin closed.

Imaging Evaluation

Intravenous digital subtraction angiography (DSA) was performed 14 days after aneurysm creation. Briefly, a 24-gauge angiocath was placed in the left ear vein and an external sizing marker was placed over the chest. During two frames per second DSA, 7 mL of iodinated contrast material was infused into the left ear vein catheter. Filming was carried into the arterial phase. Magnified views of the aneurysm cavity and adjacent artery in the anteroposterior projection were transferred to film.

Image Interpretation

Aneurysm morphology was studied by a single neuroradiologist. The width, height, and neck diameter of the aneurysm cavities were determined in reference to the external sizing device. Measurements were performed with digital calipers (Digomatic Calipers; Mitutoyo Corp, Kanagowa, Japan). The width of the aneurysm cavity was determined at its point of maximum measurement, while the height was measured from the aneurysm dome to the mid portion of a line connecting the proximal and distal portions of the aneurysm neck. The diameter of the parent artery was measured just proximal to the neck of the aneurysm (Fig 1). Aneurysms were characterized by size based on maximal diameter as small (2.0–4.9 mm), medium-sized (5.0–9.9 mm), or large (10–16 mm), and the necks of the aneurysms were characterized as small (diameter, <4 mm) or wide-necked (diameter, >4 mm). Dome-neck ratio was measured using the dome width.

Results

All animals survived aneurysm creation, and none showed any clinical evidence of neurologic insult. All aneurysms were angiographically patent at 2 weeks. The aneurysm cavities rested at the apex of a curve along the brachiocephalic artery. Most aneurysms were oblong in shape, with height greater than width.

Three (7.5%) of 40 aneurysms were small, 20 (50%) were medium-sized, and 17 (42.5%) were large. Widths of aneurysm cavities ranged from 2.5 to 7.1 mm (mean, 4.1 $\pm$ 1.2 mm) and heights ranged from 3.0 to 15.6 mm (mean, 8.8 $\pm$ 2.6 mm) (Fig 2).

Twenty-two (55%) of 40 aneurysms were small-necked, and 18 (45%) were large-necked. Twenty (50%) of 40 aneurysms had a dome-neck ratio greater than 1.0 (50%). The average dome-neck ratio was 1.13 $\pm$ 0.54. Mean parent artery diameter was 4.3 $\pm$ 1.4 mm.

Discussion

In this study we characterized the size of elastase-induced saccular aneurysms in rabbits and found excellent homology between these experimental aneurysms and ruptured, intracranial aneurysms in humans. Aneurysm dimensions in our series ranged from 3.0 to 15.6 mm. The mean width was 4.1 mm and mean height was 8.8 mm. Kassell and Torner (10), in a study characterizing the maximal diameter of ruptured aneurysms in 678 patients, found a mean maximal diameter of 8.2 mm, which is nearly identical to that seen in our experimental aneurysms. The distribution of aneurysm size was similar between our experimental aneurysms and the clinical study. Specifically, 50% of experimental aneurysms were characterized as medium-sized as compared with 58% seen clinically. This homology in size supports the use of the elastase-induced saccular aneurysm model in rabbits for preclinical testing of aneurysm occlusion devices.

In addition to aneurysm size, we also characterized the width of aneurysm necks. These data are considered important because previous literature has suggested that the absolute diameter of the aneurysm neck is critical in determining whether GDC treatment results in aneurysm occlusion (11). Zubillaga et al (11) found that 85% of aneurysms that had necks measuring less than 4 mm were occluded at a mean follow-up time of 5.6 months.

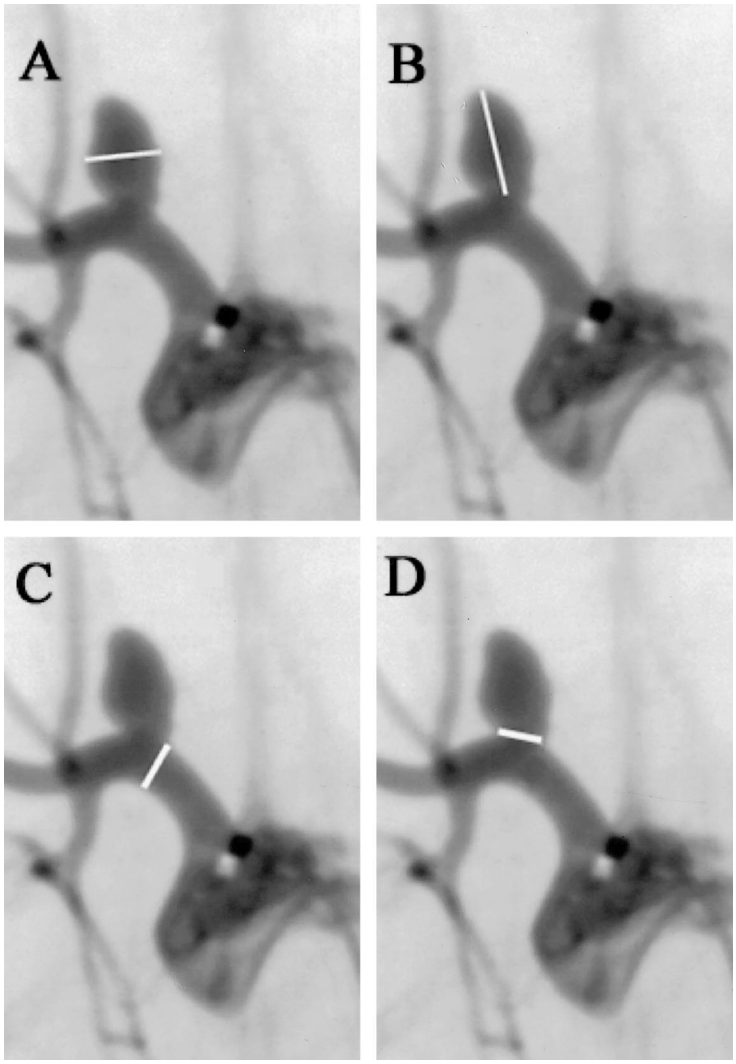

FIG 1. *A–D,* Digital subtraction angiograms in a rabbit 2 weeks after experimental aneurysm creation. The method of measurement of the aneurysm width (*A*), height (*B*), parent artery (*C*), and neck (*D*) is demonstrated.

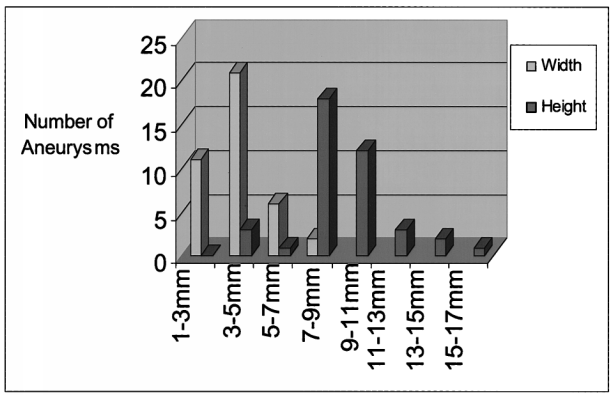

FIG 2. Graph shows range of dome sizes of experimental aneurysms.

Conversely, only 15.7% of aneurysms with necks greater than 4 mm were occluded. In experimental aneurysms, the average neck size was 3.9 ± 1.1 mm. Twenty-two (55%) of 40 experimental aneurysms were small-necked (<4 mm) and 18 (45%) were wide-necked (>4 mm). This provides a sufficient range of neck sizes to test and challenge the effectiveness of new endovascular aneurysm occlusion devices.

Dome-neck ratio has been used in the past to determine the potential for endovascular treatment. It has been suggested that a dome-neck ratio of greater than 1.0, denoting a small neck relative to the aneurysm dome, allows for endovascular therapy. In an analysis of the geometry of human saccular intracranial aneurysms, Parlea et al (12) obtained detailed measurements of 87 cerebral aneurysms. They calculated the average dome-neck ratio in ruptured aneurysm to be 1.99 ± 1.02. Our experimental aneurysms had smaller dome-neck ratios than those seen in the clinical series. This feature of low dome-neck ratios in the model may be beneficial, since wide-necked aneurysms are more difficult than narrow-necked aneurysms to treat using endovascular techniques. As new therapies for wide-necked aneurysms are developed, our model might serve as an appropriate vehicle for preclinical testing, since it renders dome-neck ratios as low as 0.8.

Morphologic characterization of our model also included the size of the adjacent parent artery. The

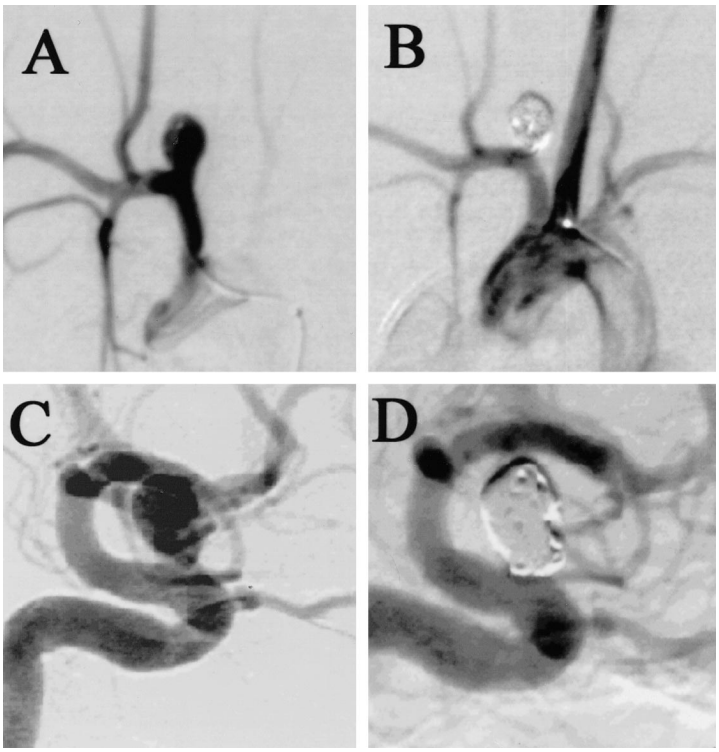

FIG 3. *A–D,* Digital subtraction angiograms show an experimental aneurysm in a rabbit before (*A*) and after (*B*) GDC placement. Note the similarity to a human ophthalmic segment aneurysm before (*C*) and after (*D*) GDC placement.

mean diameter of the brachiocephalic artery in our series was 4.3 mm, which is similar to that of human internal carotid arteries (13). This similarity in diameter of parent arteries between our model and human aneurysms facilitates testing of such treatments as balloon remodeling, in which a balloon is temporarily inflated in the parent artery across the aneurysm neck while coils are deployed.

Although simple measurements of aneurysm and parent artery diameters have confirmed similarity in size between experimental and human aneurysms, other important morphologic features are difficult to quantify. For instance, most human aneurysms occur at vessel bifurcations or along vessel curves, such as seen in ophthalmic aneurysms. Our model aneurysm occurs along the superior aspect of the brachiocephalic artery, with resultant similarity to ophthalmic artery aneurysms (Fig 3), but this similarity is difficult to quantify. Data have been published regarding experience in creation of aneurysms at the origin of the left CCA, which results in saccular aneurysms at a true bifurcation (3). However, for most of our preclinical testing of devices, we rely on the right CCA model described here, because the right CCA model is substantially easier to catheterize than the left CCA model (unpublished observation).

Even though our technique for aneurysm creation was constant throughout this study, we noted variability in aneurysm dome size, aneurysm neck diameter, and parent artery size. It has previously been demonstrated that aneurysm size does not change significantly when elastase dose or elastase incubation time is doubled (Kallmes et al, unpublished data, 1999). Parent artery dilatation was most likely due to vessel exposure to elastase, either via leakage around the Fogarty balloon at the time of intubation or from prolonged washout of elastase from the occluded CCA. Even though we cannot easily explain the cause of variation in aneurysm size, we consider this variability an advantage, as it mirrors the variability of human aneurysms and facilitates preclinical testing of aneurysm occlusion devices in a wide range of aneurysm morphologies.

Previous reports have detailed angiographic and histologic analysis of the elastase-induced aneurysm model in rabbits before and after coil embolization. Untreated aneurysms remain patent indefinitely and have a thinned elastic lamina and a continuous endothelial layer along their dome (3, 8). Coil-embolized aneurysms show only loose connective infiltration up to 3 months (9). Because of these previous reports, we have included only angiographic data in this current study, since our focus was to compare our data with human aneurysm morphology.

Beyond considerations of morphologic and histologic similarity to human aneurysms, animal models of aneurysms ideally would be easy to create and would allow endovascular treatment with standard, commercially available products. Our technique of aneurysm creation can be mastered quickly, even by practitioners with little or no surgical training. Aneurysm creation surgery is rapid, often performed in 30 minutes or less. Catheterization can be performed from the femoral route using sheaths up to 6F. We acknowledge that tortuosity of feeding vessels in rabbits cannot mimic that seen in the carotid siphon in humans. However,

even in swine and canine carotid sidewall aneurysms, the course from the femoral access site to the carotid aneurysm is nearly perfectly straight.

Conclusion

Aneurysms were reliably created using distal vessel ligation and elastase injury, and sizes of resultant aneurysms were similar to those of human intracranial aneurysms. Neck sizes varied with both large- and small-necked aneurysms created.

References

1. Cognard C, Weill A, Spelle L, et al. **Long-term angiographic follow-up of 169 intracranial berry aneurysms occluded with detachable coils.** *Radiology* 1999;212:348–356
2. Bavinzski G, al-Schameri A, Killer M, et al. **Experimental bifurcation aneurysm: a model for in vivo evaluation of endovascular techniques.** *Neurosurgery* 1998;41:129–132
3. Cloft HJ, Altes TA, Marx WF, et al. **Endovascular creation of an in vivo bifurcation aneurysm model in rabbits.** *Radiology* 1999;213:223–228
4. Massoud TF, Guglielmi G, Ji C, Vinuela F, Duckwiler GR. **Experimental saccular aneurysms, I: review of surgically-constructed models and their laboratory applications.** *Neuroradiology* 1994;36:537–546
5. Miskolczi L, Guterman LR, Flaherty JD, Szikora I, Hopkins LN. **Rapid saccular aneurysm induction by elastase application in vitro.** *Neurosurgery* 1997;41:220–228
6. Stehbens WE. **Histological changes in chronic experimental aneurysms surgically fashioned in sheep.** *Pathology* 1997;29: 374–379
7. van Alphen HA, Gao YZ, Kamphorst W. **An acute experimental model of saccular aneurysms in the rat.** *Neurol Res* 1990;12: 256–259
8. Altes TA, Cloft HJ, Short JG, et al. **Creation of saccular aneurysms in the rabbit: a model suitable for testing endovascular devices.** *AJNR Am J Neuroradiol* 2000;174:349–354
9. Kallmes DF, Helm GA, Hudson SB, et al. **Histologic evaluation of platinum coil embolization in an aneurysm model in rabbits.** *Radiology* 1999;213:217–222
10. Kassell NF, Torner JC. **Size of intracranial aneurysms.** *Neurosurgery* 1983;12:291–297
11. Zubillaga AF, Guglielmi G, Vinuela F, Duckwiler G. **Endovascular occlusion of intracranial aneurysms with electrically detachable coils: correlation of aneurysm neck size and treatment results.** *AJNR Am J Neuroradiol* 1994;15:815–820
12. Parlea L, Fahrig R, Holdsworth DW, Lownie SP. **An analysis of the geometry of saccular intracranial aneurysms.** *AJNR Am J Neuroradiol* 1999;20:1079–1089
13. Kane AG, Dillon WP, Barkovich AJ, Norman D, Dowd CF, Kane TT. **Reduced caliber of the internal carotid artery: a normal finding with ipsilateral absence or hypoplasia of the A1 segment.** *AJNR Am J Neuroradiol* 1996;17:1295–1301